Valley-dependent two-dimensional transport in (100), (110), and (111) Si inversion layers at low temperatures and carrier densities

E. H. Hwang[1,2] and S. Das Sarma[1]

[1]*Condensed Matter Theory Center, Department of Physics, University of Maryland, College Park, Maryland 20742-4111, USA*

[2]*SKKU Advanced Institute of Nanotechnology, Sungkyunkwan University, Suwon 440-746, Korea*

(Received 14 October 2012; revised manuscript received 14 January 2013; published 7 February 2013)

Motivated by interesting recent experimental results, we consider theoretically charged-impurity scattering-limited two-dimensional (2D) electronic transport in (100), (110), and (111)-Si inversion layers at low temperatures and carrier densities, where screening effects are important. We show conclusively that, given the same bare Coulomb disorder, the 2D mobility for a given system increases monotonically with increasing valley degeneracy. We also show that the temperature and the parallel magnetic field dependence of the 2D conductivity is strongly enhanced by increasing valley degeneracy. We analytically consider the low-temperature limit of 2D transport, particularly its theoretical dependence on valley degeneracy, comparing with our full numerical results and with the available experimental results. We make qualitative and quantitative predictions for the parallel magnetic field induced 2D magnetoresistance in recently fabricated high-mobility 6-valley Si(111)-on-vacuum inversion layers. We also provide a theory for 2D transport in ultrahigh mobility Si(111) structures recently fabricated in the laboratory, discussing the possibility of observing the fractional quantum Hall effect in such Si(111) structures.

DOI: 10.1103/PhysRevB.87.075306 PACS number(s): 73.40.−c, 72.10.−d, 72.20.Dp

I. INTRODUCTION

Many semiconductor-based two-dimensional (2D) electron systems have an intrinsic valley degeneracy (g_v) in addition to the spin degeneracy ($g_s = 2$). This valley degeneracy, which arises from the bulk band structure of the corresponding three-dimensional (3D) material, is usually exact within the effective mass approximation, but is only approximate in the experimental 2D systems where there could be small energy level splittings between different valleys (the so-called "valley splitting").[1] If the valley splitting is "small" in some operational sense, the 2D system could be considered to have a total quantum degeneracy of $g = g_s g_v$ with both spin and valley states being quantum degenerate. A well-known example of valley degeneracy is graphene, which has a valley degeneracy of $g_v = 2$ with equivalent Dirac cones at K and K' points of the Brillouin zone.[2] Examples of semiconductor-based 2D electron systems with valley degeneracy $g_v(>1)$ are Si(100), (110), and (111) electron inversion layers in MOSFETs[1] as well as AlAs- and AlSb-based 2D electron systems.[3,4] Many other 2D systems (e.g., n-GaAs and p-GaAs 2D electron and hole systems) have no valley degeneracy ($g_v = 1$).[3] Valley degeneracy obviously has a profound effect on the electronic properties of the 2D system.

The purpose of the current paper is a systematic theoretical investigation of the valley degeneracy effect on 2D electronic transport properties, using Si-MOSFET-structure-based n-inversion layers as the specific system under consideration (since these typically have $g_v > 1$) although our qualitative and analytical results would apply to all 2D semiconductor systems (specifically Si-Ge 2D electron systems) with $g_v \geqslant 1$. Transport properties of 2D systems (e.g., Si-MOSFETs, GaAs heterostructures, and quantum wells, SiGe-based 2D structures) have been studied extensively over the last 25 years[5–8] because of the experimental observation of an apparent metallic behavior in the high-mobility low-density electron inversion layer in Si-MOSFET structures.[9] Many theoretical interpretations of the experimentally observed apparent metallic behavior (i.e., so-called metal-insulator transition) in 2D systems have been proposed.[8,10–12] However, in this paper we do not make any attempt to discuss the 2D metal-insulator transition (MIT) literature. Our goal in this paper is to provide a systematic theoretical investigation of the valley degeneracy effect on 2D electronic transport properties, which have not been discussed in literature to the best of our knowledge.

The valley-dependent electronic properties of a 2D (or 3D for that matter) semiconductor system is best understood by considering the electronic density of states in the valley-degenerate ground state, which is given for the 2D (3D) system by $D(\epsilon) = gm/2\pi\hbar^2$ $(g\sqrt{\epsilon}(2m)^{3/2}/4\pi^2\hbar^3)$, where $g = g_s g_v$ is the ground-state degeneracy arising from both spin (g_s) and valley (g_v) degeneracies. The linear proportionality of the electronic density of states with the valley degeneracy leads immediately to the following dependencies of the Fermi wave vector (k_F), the Thomas-Fermi screening wave vector ($q_{\rm TF}$), and the Fermi energy (E_F) on the valley degeneracy in 2D and 3D systems:

$$k_F \sim g_v^{-1/2} \ \text{(2D)}; \quad g_v^{-1/3} \ \text{(3D)}, \tag{1a}$$

$$q_{\rm TF} \sim g_v \ \text{(2D)}; \quad g_v^{2/3} \ \text{(3D)}, \tag{1b}$$

$$\epsilon_F \sim g_v^{-1} \ \text{(2D)}; \quad g_v^{-2/3} \ \text{(3D)}. \tag{1c}$$

Since $D(\epsilon)$, k_F, $q_{\rm TF}$, and ϵ_F all depend nontrivially on the valley degeneracy factor g_v, all electronic properties, including 2D transport properties, depend nontrivially on the valley degeneracy. We note that the valley-dependent transport properties are in general nontrivial since g_v enters independently through both $q_{\rm TF}$ (and hence screening) and k_F (and hence scattering wave vector). Increasing (decreasing) the valley degeneracy enhances (suppresses) screening through

q_{TF}, but at the same time it also affects k_F, increasing it with decreasing g_v.

Bulk Si has six equivalent conduction band minima located about 85% to the Brillouin zone boundary, thus making bulk Si a $g_v = 6$ system. Each valley corresponds to an ellipsoid with anisotropic effective mass along and perpendicular to the symmetry axes. There are thus three possible Si-based 2D electron systems, depending on whether (100), (110), or (111) surface is used for creating the 2D confinement. Within the effective mass approximation these three distinct 2D Si systems have different valley degeneracies: $g_v = 2$ [Si(100)], 4 [Si(110)], and 6 [Si(111)]. Uniaxial stress would lift the fourfold or the sixfold valley degeneracy of Si(110) or (111) system, making the ground state of each a doubly degenerate $g_v = 2$ system similar to the Si(100) system (but, of course, with a distinct effective mass for each 2D system). It is important to mention in this context the fact that essentially all Si-based 2D systems studied in the literature have experimentally manifested $g_v = 2$, even for Si(110) and (111) systems which nominally should have $g_v = 4$ and 6, respectively. This is thought to be due to extensive random uniaxial stress universally present at the Si-SiO_2 interface in Si-MOSFET structures, which pulls down two equivalent valleys compared with the other valleys, making both Si(110) and Si(111) MOSFETs to have doubly degenerate ground states ($g_v = 2$) similar to the Si(100) MOSFETs (but with different effective masses). An early experiment[13] did manage to observe a sixfold valley degeneracy in Si(111)-SiO_2 MOSFETs, but the system had very poor mobility and was not useful for the investigation of valley-dependent transport properties. Other than this one exception,[13] all Si-SiO_2 2D MOSFETs invariably manifest $g_v = 2$ ground state, independent of their surface orientation in sharp contrast to the effective mass-approximation-based expectation of $g_v = 6$ (4) for Si(111) [(110)] systems.

An exciting new experimental development in the subject, which is the direct motivation for our study, is the recent fabrication of very high-quality Si(111)-on-vacuum 2DEG FET structures,[14,15] which exhibit $g_v = 6$ ground state in agreement with the Si bulk band structure effective mass approximation. Presumably the very high quality (without any interface strain) of the Si-vacuum interface, leading to very high mobility ($\sim 10^5$ cm^2/Vs), produce the expected sixfold valley degeneracy. The fact that these Si-vacuum 2D FET systems also have very high mobility is consistent with the high quality of the Si surface leading to the $g_v = 6$ Si(111) 2D system. The absence of a Si-SiO_2 interface may be the reason that these new Si-vacuum-based 2D systems satisfy the expected $g_v = 6$ effective mass approximation prediction. The absence of a real solid interface may simply enable the bulk effective mass approximation to be valid at the surface leading to the Si(111) sixfold degeneracy. Although similar 2D systems on the Si(110)-vacuum system have not yet been made, it is reasonable to expect that the corresponding Si(110) 2D system will have $g_v = 4$ valley degeneracy. Recently, the transport properties of Si(111) with sixfold valley degeneracy have been discussed.[16–18] We note that these Si-vacuum 2D systems manifest, in addition to the expected valley degeneracy anticipated on the basis of the effective mass approximation, also extremely high 2D mobilities because of the lack of random impurities in the oxide layer which adversely affects the mobility in the Si-SiO_2 2D systems.

In particular, of course, the effective mass approximation is not exact and breaks down at an interface.[19] Thus, even the double degeneracy ($g_v = 2$) of the Si(100) 2D system [or of the Si(110) and (111) systems as observed experimentally] is only approximate and is lifted beyond the simple effective mass approximation leading to small (<1 meV) energy splitting between the two valleys. One can, therefore, think about an experimental single valley 2D Si system where this ground-state valley splitting is large enough so that the higher valley state is not occupied by electrons. Thus, in principle, the valley degeneracy of Si-based 2D MOSFET or inversion layer system for any surface orientation can be thought to be a continuous variable ranging between 1 and 6 depending on the microscopic details of the interface. This is the approach we take in the current work where g_v is assumed to be free parameters to be determined experimentally.

Motivated by the above considerations, we theoretically consider valley-dependent 2D transport in Si systems assuming the valley degeneracy g_v to be a free rational variable—in reality, of course, g_v can only be 1, 2, 4, or 6 in Si 2D systems depending on the situation. We address the density, the temperature, and the in-plane magnetic field dependence of 2D transport in the presence of a variable valley degeneracy. The applied in-plane magnetic field is parallel to the 2D system and is therefore assumed to only affect the spin degeneracy of the 2DEG since it gives rise to a Zeeman splitting between up/down spin levels. We find remarkably strong valley dependence of 2D transport properties, and believe that the interesting physics of valley-dependent 2D transport should be investigated experimentally. The recently fabricated high-mobility Si-vacuum 2D electron systems[14,15] should be particularly suitable in this context.

We organize the rest of this article as follows: In Sec. II we provide the detailed transport theory and a background giving a physical picture for why 2D carrier transport should depend strongly on the valley degeneracy, followed by the numerical results (III). In Sec. IV we provide our calculated mobility for the recently fabricated extreme high-mobility Si(111) 2D samples. We conclude in Sec. V with a discussion.

II. TRANSPORT THEORY

To calculate the density, temperature, and in-plane magnetic field dependence of 2D conductivity, $\sigma(T,n,B_{||})$, we use the Drude-Boltzmann semiclassical theory for 2D transport limited by screened charged impurity scattering.[1,7] We assume that the 2D carrier conductivity is entirely limited by screened impurity scattering, where the disorder arises from randomly distributed charged impurities in a 2D plane located at the interface between Si-SiO_2 (or Si-vacuum) and random background charged impurity centers (i.e., unintentional dopants) in the 2D layer itself. We neglect all phonon scattering effects as well as surface roughness scattering. In the low-temperature limit (e.g., $T < 10$ K regime of interest to us) phonon scattering is negligible for 2D electrons in MOSFET structures and the short-range surface roughness scattering at the Si-SiO_2 interface is only important in the high-density limit ($n > 10^{12}$cm^{-2}) (the roughness scattering can be neglected

in Si-vacuum systems).[16,20] At low carrier densities ($n < 10^{12}$ cm^{-2}) and at low temperatures ($T < 10$ K) the 2D transport in Si-MOSFETs is dominated by the long-range Coulomb scattering by unintentional random charged impurities present at the Si-insulator interface and background unintentional dopants inside Si. The background impurity density is low ($\sim 10^{16}$cm^{-3}), but it may dominate all other scattering in high-mobility Si-vacuum systems since the interface scattering is strongly suppressed due to the absence of the oxide layer.

The 2D conductivity is given in the Boltzmann theory by

$$\sigma = e^2 \int d\epsilon D(\epsilon) \frac{v_k^2}{2} \tau(\epsilon) \left[-\frac{\partial f(\epsilon)}{\partial \epsilon} \right], \tag{2}$$

where $D(\epsilon) = gm/(2\pi\hbar^2)$ is the density of states with total degeneracy $g = g_s g_v$ and the carrier effective mass m, $v_k = \hbar k/m$ is the carrier velocity, $\epsilon = (\hbar k)^2/2m$ is the usual parabolic 2D electron energy dispersion, $f(\epsilon)$ is the Fermi distribution function, and $\tau(\epsilon)$ is the energy-dependent transport relaxation time.

At $T = 0$ we have $\sigma = ne^2\tau(\epsilon_F)/m$, where $n = gk_F^2/4\pi$ is the 2D carrier density with k_F being the Fermi wave vector and ϵ_F the Fermi energy. At finite temperatures we can express Eq. (2) by keeping the total carrier density constant $\sigma = ne^2\langle\tau\rangle/m$, where the energy averaged transport relaxation time $\langle\tau\rangle$ is given by

$$\langle\tau\rangle = \frac{\int d\epsilon \epsilon \tau(\epsilon) \left[-\frac{\partial f(\epsilon)}{\partial \epsilon} \right]}{\int d\epsilon \epsilon \left[-\frac{\partial f(\epsilon)}{\partial \epsilon} \right]}. \tag{3}$$

In the Born approximation the transport scattering time is given by considering screened charged impurity centers,

$$\frac{1}{\tau(\epsilon_{\mathbf{k}})} = \frac{2\pi}{\hbar} \int dz \int \frac{d^2k'}{(2\pi)^2} N_i(z) \left| \frac{U^i(\mathbf{q},z)}{\varepsilon(q)} \right|^2 \times (1 - \cos\theta_{\mathbf{k}\mathbf{k}'}) \delta(\epsilon_{\mathbf{k}} - \epsilon_{\mathbf{k}'}), \tag{4}$$

where $U^i(q;z)$ is the bare Coulomb potential for electron-charged impurity interaction, $\mathbf{q} = \mathbf{k} - \mathbf{k}'$ is the momentum transfer, and $N_i(z)$ is the random charged impurity density in the direction (z) normal to the 2D plane of confinement. The $z = 0$ is the interface plane between Si and the insulator. In our model with two different kinds of impurity $N_i(z) = N_i^{3D} + n_i\delta(z - z_0)$, where N_i^{3D} is the background 3D charged impurity density and n_i is the 2D charged impurity density at z_0 from the interface. In Eq. (4) $\varepsilon(q) = 1 - v(q)\Pi(q)$ is the random phase approximation (RPA)[21] dielectric screening function due to the 2D electrons themselves, where $v(q)$ is the 2D bare Coulomb interaction, and $\Pi(q) \equiv \Pi(q, T, B_\parallel)$ is the 2D finite wave-vector polarizability function depending on both temperature and spin polarization in the presence of a finite parallel magnetic field.

To understand a physical picture for why 2D carrier transport should depend strongly on the valley degeneracy we consider the conductivity for a strict 2D system at the zero temperature. However, in the realistic Si-MOSFET systems quasi-2D quantum form factor effects arising from the finite width of the 2D layer in the z direction must be included in $U^i(q;z)$ and $v(q)$. For this purpose the usual Howard-Fang variational function[22] is used in our numerical calculations. We will show that the quantum form factor effects are of considerable quantitative importance especially at low densities, where the system cannot really be thought of as an almost zero-width 2D layer.

Using 2D RPA screening function at $T = 0$ we have the scattering time for charged impurity centers,

$$\frac{1}{\tau(\epsilon_F)} = 2\pi\hbar \frac{n_i}{m} \left(\frac{2}{g} \right)^2 q_0^2 I(q_0), \tag{5}$$

where $q_0 = q_{TF}/2k_F \propto g_v^{3/2}$ ($q_{TF} = g/a_B$ is a 2D Thomas-Fermi wave vector with effective Bohr radius $a_B = \hbar^2\kappa/me^2$ where κ is the background dielectric constant), and $I(q_0)$ is given by

$$I(q_0) \approx \pi + [2 + 4\log(q_0/2)]q_0 \quad \text{for } q_0 \ll 1, \qquad \approx \frac{\pi}{2q_0^2} \quad \text{for } q_0 \gg 1. \tag{6}$$

Thus in the strong screening limit (or $q_0 \gg 1$) we have $\tau^{-1}(\epsilon_F) = \pi^2\hbar\frac{n_i}{m}(\frac{2}{g})^2 \propto g_v^{-2}$, and the conductivity becomes $\sigma \propto g_v^2$, i.e., the conductivity increases quadratically with g_v. In the opposite limit (i.e., weak screening limit, $g_0 \ll 1$) we have $\tau^{-1}(\epsilon_F) = 2\pi^2\hbar\frac{n_i}{m}(\frac{2}{g})^2 q_0^2 \propto g_v$, and the conductivity becomes $\sigma \propto g_v^{-1}$. In general, the effective screening (q_0) of a 2D system becomes stronger as the density decreases. For Si(100) samples, $q_0 \approx 4.7g^{3/2}/\sqrt{\tilde{n}}$, where $\tilde{n} = n/(10^{10}\text{cm}^{-2})$. Thus, for the density regime of interest to us, $n < 10^{12}$cm^{-2}, $q_0 \gg 1$ and the transport of 2D Si systems depends strongly (quadratically) on the valley degeneracy.

At finite temperatures ($T < T_F$, where $T_F = \epsilon_F/k_B$ is the Fermi temperature), the leading order correction to the conductivity is linear in temperature and given by[7]

$$\sigma(T) \sim \sigma_0 \left[1 - \frac{2q_0}{1 + q_0} \frac{T}{T_F} \right], \tag{7}$$

where $\sigma_0 = \sigma(T = 0)$. In the strong screening limit ($q_0 \gg 1$) we have

$$\delta\sigma/\sigma_0 \propto -g_v T/n, \tag{8}$$

where $\delta\sigma = \sigma(T) - \sigma_0$. On the other hand, in the weak screening limit we have

$$\delta\sigma/\sigma_0 \propto -g_v^{5/2} T/n^{3/2}. \tag{9}$$

Thus for $q_0 \gg 1$ the conductivity decreases linearly with valley degeneracy for fixed temperature and density, but for $q_0 \ll 1$ it decreases as $g_v^{5/2}$.

Since there are two different carrier components (spin up and down) in the presence of a finite parallel magnetic field the total conductivity of the partially polarized system is given by $\sigma = \sigma_+ + \sigma_-$, where $\sigma_\pm = n_\pm e^2\tau_\pm/m$ is the conductivity of spin up (+) and down (−), respectively. $n_\pm$ is the carrier densities of spin state $\pm$, and $\tau_\pm$ is the transport relaxation time of the spin up (down) state. To calculate the conductivity with screened charged impurities in the presence of parallel magnetic field, spin-polarization effects must be included in the polarizability.[23,24] When the parallel magnetic field is applied to a 2D electron system the polarizability becomes $\Pi_{tot}(q) = \Pi_+(q) + \Pi_-(q)$, where $\Pi_\pm(q)$ is the polarizability of the spin up (down) state and is given by at $T = 0$,

$$\Pi_\pm(q) = D_F[1 - \sqrt{1 - (2k_F^\pm/q)^2}\theta(q - 2k_F^\pm)], \tag{10}$$

where $D_F = g_v m/2\pi$, g_v is the valley degeneracy factor, and $k_F^{\pm}$ are the Fermi wave vector of the spin up (down) state.

For strictly 2D systems with zero thickness the spin polarization changes the screening function and this effect gives rise to positive (negative) magnetoresistance in the strong (weak) screening limits.[23,24] In the strong screening limit ($q_0 \gg 1$) $\sigma(B_s)/\sigma(0) \approx 1/4$ and in the weak screening limit ($q_0 \ll 1$) $\sigma(B_s)/\sigma(0) \sim 2$, where $\sigma(0) = \sigma(B = 0)$ and B_s is the magnetic field for complete spin polarization. Since the valley degeneracy affects the screening strength q_0 it is expected that the positive magnetoresistance is enhanced as g_v increases. If we include the finite width confinement effect in the calculation the ratio becomes much smaller, especially at low density. In addition to the screening effects in the impurity potential, for the real systems with finite width confinement the orbital effects[25] dominate over spin effects at large magnetic fields. However we neglect the orbital effects in this paper, which has been considered elsewhere.[25]

III. RESULTS

Throughout this paper we use the following parameters: The dielectric constants of Si, SiO_2, and vacuum are $\kappa_{Si} =$ 11.7, $\kappa_{SiO_2} = 3.9$, and $\kappa_{vac} = 1$, respectively, and the effective masses corresponding to the Si surface of (100), (110), and (111) are $m = 0.19m_e$, $m = 0.28m_e$, and $m = 0.30m_e$, respectively, where m_e is the free-electron mass. In the absence of a parallel magnetic field the spin degeneracy $g_s = 2$ is used everywhere.

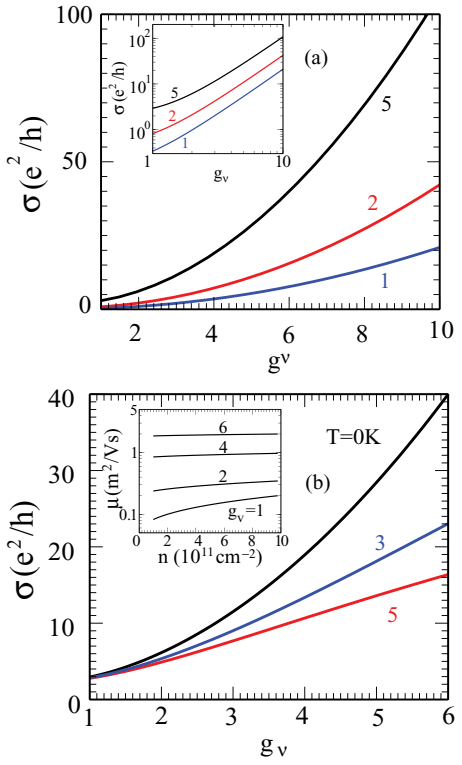

FIG. 1. (Color online) Calculated conductivity for SiO_2-Si(100) MOSFET system as a function of valley degeneracy (g_v) (a) for various electron densities n =1.0, 2.0, 5.0×10^{11} cm^{-2} (bottom to top) at $T = 0$ and (b) for a density n =5.0×10^{11}cm^{-2} and for various temperatures $T = 0$, 3, and 5 K. Inset in (a) shows the same results of (a) in logarithm scale showing $\sigma \sim g_v^2$ for large g_v. Inset in (b) shows mobility at $T = 0$ K as a function of density for different valley degeneracies, $g_v = 1$, 2, 4, 6. The parameters corresponding to Si(100) are used and the impurity density of $n_i = 3 \times 10^{11}$cm^{-2} located at the interface ($z = 0$) is used.

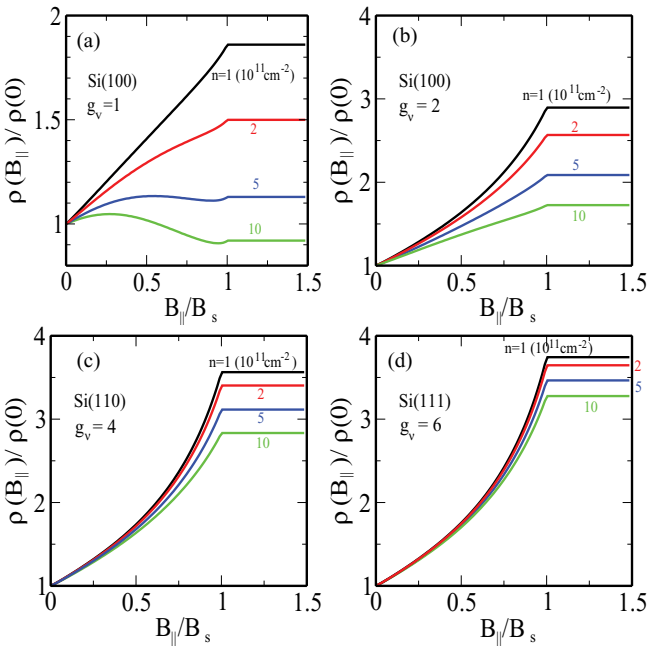

FIG. 2. (Color online) Magnetoresistivity of SiO_2-Si MOSFET systems. Magnetoresistivity ($\rho \equiv 1/\sigma$) of (a),(b) Si(100) ($g_v = 1$, $g_v = 2$), (c) Si(110) ($g_v = 4$), and (d) Si(111) ($g_v = 6$) MOSFET systems for various electron densities n =1.0, 2.0, 5.0, 10.0×10^{11}cm^{-2} (top to bottom). Impurities are located at the interface $z = 0$. Here $\rho(0)$ is the resistivity at $B = 0$ and B_s is the magnetic field for complete spin polarization, i.e., $g_s = 2$ at $B = 0$ and $g_s = 1$ at $B \geqslant B_s$.

In Fig. 1(a) we show our calculated zero magnetic field conductivity of SiO_2-Si(100) MOSFETs as a function of valley degeneracy (g_v) for various electron densities n =1.0, 2.0, 5.0×10^{11} cm^{-2} (bottom to top) at $T = 0$, by assuming that the impurities with density $n_i = 3 \times 10^{11}$cm^{-2} are located at the interface ($z = 0$). As shown in the inset of Fig. 1(a) in logarithm scale, the calculated conductivity increases as $\sigma(g_v) \propto g_v^{\alpha}$, where α increases as g_v increases and approaches 2 which is expected in the strong screening limit. In Fig. 1(b) the conductivity is shown as a function of g_v for a density $n = 5.0 \times 10^{11}$cm^{-2} and for various temperatures $T = 0$, 3, and 5 K with the same parameters as Fig. 1(a). We see that the temperature dependence of conductivity becomes stronger since the conductivity decreases linearly with g_v for a fixed density and temperature in the strong screening limits [see. Eq. (8)].

In Figs. 2 and 3 we show the calculated resistivity ($\rho = 1/\sigma$) for SiO_2-Si MOSFET systems assuming that all impurities are located at the interface $z = 0$. In Fig. 2 magnetoresistivity for (a), (b) Si(100) with $g_v = 1$, $g_v = 2$, respectively, (c) Si(110) with $g_v = 4$, and (d) Si(111) with $g_v = 6$ MOSFET systems are shown for various electron densities n =1.0, 2.0, 5.0, 10.0×10^{11}cm^{-2} (top to bottom).

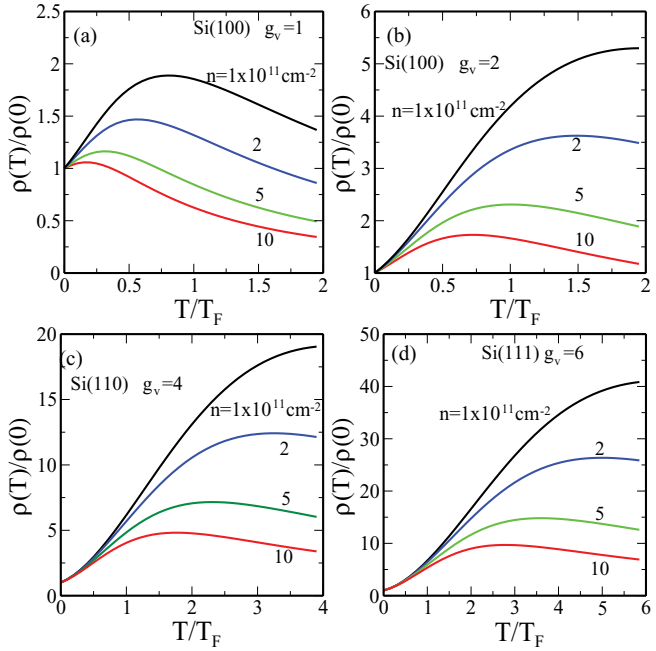

FIG. 3. (Color online) Resistivity of SiO_2-Si MOSFET systems. Temperature-dependent resistivity of (a),(b) Si(100) ($g_v = 1$, $g_v = 2$), (c) Si(110) ($g_v = 4$), and (d) Si(111) ($g_v = 6$) MOSFET systems for various electron densities n =1.0, 2.0, 5.0, 10.0 $\times 10^{11}$cm^{-2} (top to bottom). Here $\rho(0)$ is the resistivity at $T = 0$ and T_F is the Fermi temperature, $T_F = E_F/k_B$. The same parameters as Fig. 2 are used.

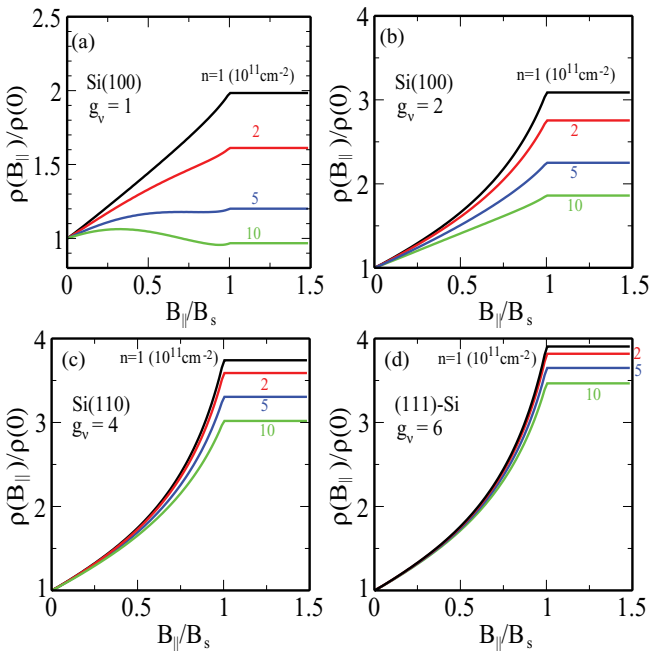

FIG. 4. (Color online) Vacuum-Si MOSFET systems. Magnetoresistivity of (a), (b) Si(100) ($g_v = 1$, $g_v = 2$), (c) Si(110) ($g_v = 4$), and (d) Si(111) ($g_v = 6$) MOSFET systems for various electron densities n =1.0, 2.0, 5.0, 10.0 $\times 10^{11}$cm^{-2} (top to bottom). All impurities are located at the interface $z = 0$.

$\rho(0)$ is the resistivity at $B = 0$ and B_s is the magnetic field for complete spin polarization, i.e., $g_s = 2$ at $B = 0$ and $g_s = 1$ at $B \geqslant B_s$. As expected the ratio $\rho(B_s)/\rho(0)$ is close to 4 for larger g_s systems due to the enhancement of effective screening. Because of the finite confinement effects the ratio $\rho(B_s)/\rho(0)$ is smaller than that of strict 2D system. Note that the results for Si(110) and Si(111) with $g_v = 2$ is very close to the results of Fig. 2(b) even though we use the parameters corresponding to Si(110) and Si(111). The results for Si(111) with $g_v = 4$ are almost identical to the results of Fig. 2(c). The parameters corresponding to sample properties except the valley degeneracy have only a small effect on the ratio. The most important parameter determining the ratio is the screening strength q_0. For $g_v = 1$ the effective screening becomes weak, and especially at high densities, $q_0 < 1$ is expected, as a consequence, the magnetoresistance decreases as the magnetic field increases (see the result for $g_v = 1$ and $n = 10^{12}$cm^{-2}).

In Fig. 3 the temperature-dependent resistivity of (a), (b) Si(100) ($g_v = 1$, $g_v = 2$, respectively), (c) Si(110) ($g_v = 4$), and (d) Si(111) ($g_v = 6$) MOSFET systems are shown for various electron densities n =1.0, 2.0, 5.0, 10.0 $\times 10^{11}$cm^{-2} (top to bottom). Here $\rho(0)$ is the resistivity at $T = 0$ and T_F is the Fermi temperature, $T_F = E_F/k_B$. As shown in Eq. (8) at low temperatures $T < T_F$ the metallic behavior [i.e., $d\rho(T)/dT > 0$] is strong for larger g_v and at small densities. Thus, a stronger metallic behavior is expected for Si(111) with $g_v = 6$.[16] For $g_v = 1$ effective screening is weak, i.e., $q_0 = q_{TF}/2k_F < 1$, and strong-screening condition can only be satisfied at very low carrier densities. Thus, we expect rather weak temperature and field dependence of resistivity for $g_v = 1$ except at very low densities. Figure 3 shows the very interesting feature that the crossover temperature (i.e., the temperature at maximum resistivity) is almost independent of g_v. Since $T_F \propto g_v/n$, the scaled crossover temperature (T/T_F) increases as the valley degeneracy increases for a fixed density, but the absolute crossover temperature is very close for all g_s values.

In Figs. 4 and 5 we show the calculated resistivity, $\rho(B_{\|})$ and $\rho(T)$, respectively, for vacuum-Si MOSFET systems assuming that all impurities are located at the interface $z = 0$. In the calculation of resistivity for vacuum-Si MOSFETs we use the same parameters and the same impurity configuration for SiO_2-Si MOSFETS, except the insulating dielectric constant (SiO_2 vs vacuum, i.e., κ_{SiO_2} vs κ_{vac}), for direct comparison with the results of SiO_2-Si MOSFETs (Figs. 2 and 3). Since the screening strength q_0 is inversely proportional to the background dielectric constant at the same carrier density both magnetic-field-dependent and temperature-dependent resistivity for vacuum-Si MOSFETs is stronger than for SiO_2-Si MOSFETs as shown in Figs. 4 and 5. However, overall behaviors for both systems are very similar if we assume that the impurity configurations are identical. But in reality the impurity configurations are very different for these two systems. In the H-passivated Si-vacuum MOSFET it is expected that interface quality between vacuum and Si is much better with substantially less interface charged impurities than in Si-SiO_2. Especially in high-mobility vacuum-Si MOSFETs it is considered that background unintentional 3D charged impurity is the most important scattering source.

In Figs. 6 and 7 we show the calculated magnetic-field- and temperature-dependent resistivity of vacuum-Si MOSFETs, $\rho(B_{\|})$ and $\rho(T)$, respectively, assuming that background charged impurities with impurity density $N_i^{3D} = 2.3 \times 10^{16}$cm^{-3} is the only scattering source (i.e., we set the

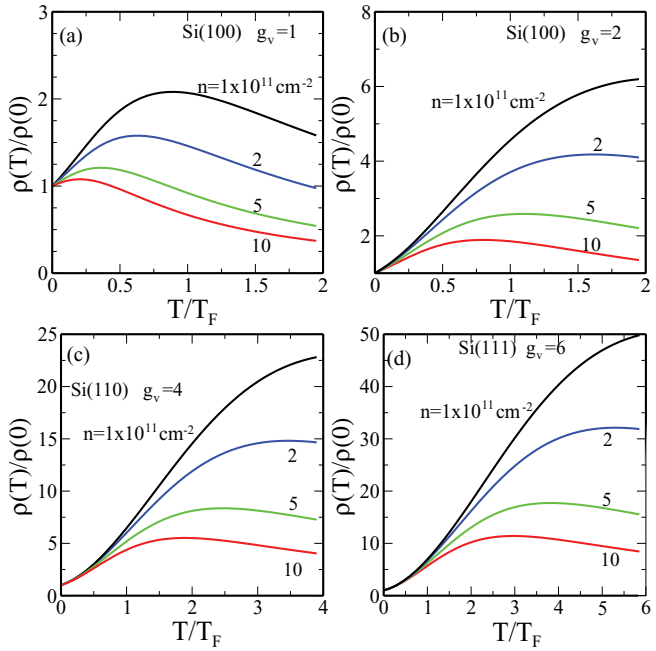

FIG. 5. (Color online) Vacuum-Si MOSFET systems. Temperature-dependent resistivity of (a),(b) Si(100) ($g_v = 1$, $g_v = 2$), (c) Si(110) ($g_v = 4$), and (d) Si(111) ($g_v = 6$) MOSFET systems for various electron densities n =1.0, 2.0, 5.0, 10.0 $\times 10^{11}$cm^{-2} (top to bottom). Calculations are done with only interface impurities. We use the same parameters as Fig. 4.

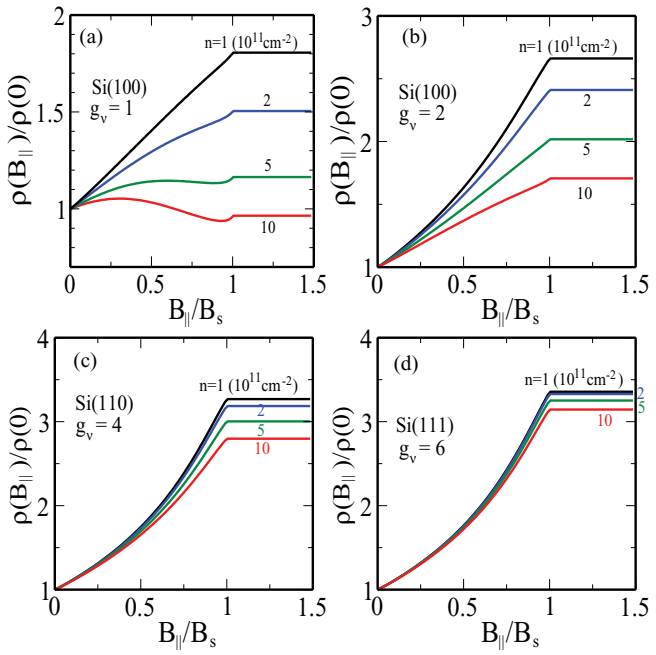

FIG. 6. (Color online) Vacuum-Si MOSFET systems. Magnetoresistivity of (a),(b) Si(100) ($g_v = 1$, $g_v = 2$), (c) Si(110) ($g_v = 4$), and (d) Si(111) ($g_v = 6$) MOSFET systems for various electron densities n =1.0, 2.0, 5.0, 10.0 $\times 10^{11}$cm^{-2} (top to bottom). Here only unintentional 3D bulk impurities are considered with density $N_i^{3D} = 2.3 \times 10^{16}$cm^{-3}.

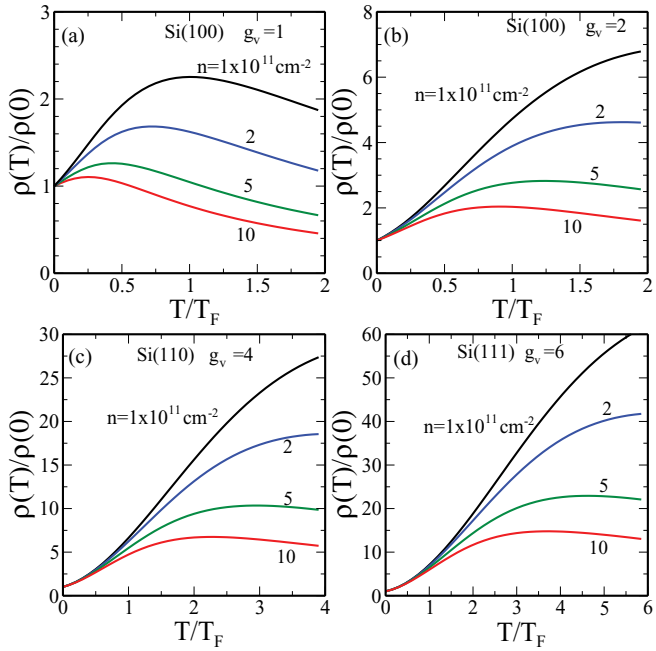

FIG. 7. (Color online) Vacuum-Si MOSFET systems. Temperature-dependent resistivity of (a),(b) Si(100) ($g_v = 1$, $g_v = 2$), (c) Si(110) ($g_v = 4$), and (d) Si(111) ($g_v = 6$) MOSFET systems for various electron densities n =1.0, 2.0, 5.0, 10.0 $\times 10^{11}$cm^{-2} (top to bottom). The same impurity configuration of Fig. 6 is used.

interface impurity $n_i = 0$). Even though the overall magnetic field and temperature dependencies of resistivity are very similar to the results of Figs. 4 and 5 (which are calculated with interface charged impurity scattering) there are substantial differences between the two different impurity configurations. Comparing Fig. 6 with Fig. 4 we find that the parallel magnetic-field dependence of resistivity calculated with background 3D impurities is weaker than that with interface impurities (Fig. 4). However the temperature dependence of resistivity calculated with 3D impurities is stronger than that with interface impurity (Fig. 5). Our predictions can be directly verified by carrying out parallel field measurements in Si-vacuum 2D systems.

IV. HIGH-MOBILITY Si(111) SYSTEM

Very recent experimental work[26] using ultraclean H-passivated Si(111)-vacuum 2D electron systems shows unprecedented high mobilities, approaching several hundred thousand cm^2/Vs at low temperatures, corresponding to a momentum relaxation time (level broadening) of 30 ps (∼0.02 meV). These mobility numbers of these recent samples surpass the old Si(111) mobilities[13] by factors of 100 and are comparable in quality (in terms of the momentum relaxation time and level broadening) to better-quality 2D GaAs electron samples where fractional quantum Hall phenomena typically manifest. Since the Si(111) 2D system is a multivalley system in contrast to the 2D GaAs system, the observation of the fractional quantum Hall effect in Si(111) 2D system is a very interesting and potentially very important new development.

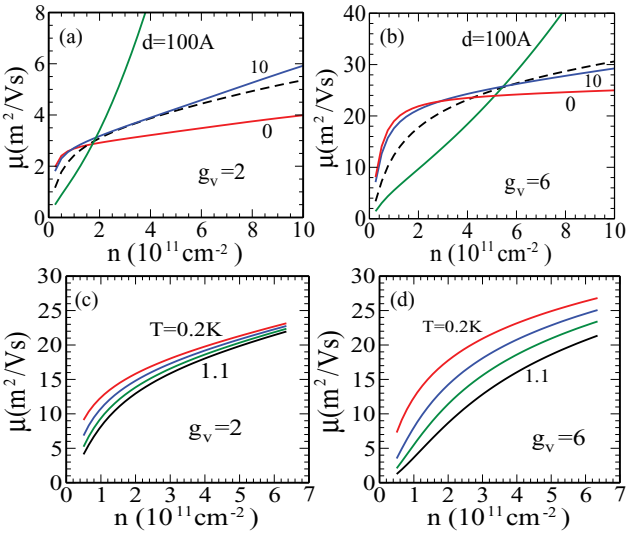

FIG. 8. (Color online) Vacuum-Si(111) MOSFET systems. The calculated density-dependent mobility for different impurity configurations at $T = 0.2$ K is shown (a) for $g_v = 2$ and (b) for $g_v = 6$. The black dashed lines represent the results with only 3D bulk impurities with $N_i^{3D} = 2.3 \times 10^{16}\text{cm}^{-3}$, and other three lines represent results with only 2D impurities (no bulk impurities): $z = 0$ Å with $n_i = 2.0 \times 10^{10}\text{cm}^{-2}$, $z = 10$ Å with $n_i = 2.4 \times 10^{10}\text{cm}^{-2}$, and $z = 100$ Å with $n_i = 21.0 \times 10^{10}\text{cm}^{-2}$. (c) and (d) show the calculated mobility with only 3D bulk charged impurities as a function of density for different temperatures $T = 0.2, 0.5, 0.8$, and 1.1 K (from top to bottom). In (c) $g_v = 2$ and the bulk 3D impurities of density $N_i^{3D} = 4.5 \times 10^{15}\text{cm}^{-3}$ are used. In (d) $g_v = 6$ and the bulk 3D impurities of density $N_i^{3D} = 2.3 \times 10^{16}\text{cm}^{-3}$ are used.

In Fig. 8 we show our numerical results (based on the theory given in Sec. II) for the low-temperature mobility (defined simply as the conductivity divided by ne, $\mu = \sigma/ne$, where n is the carrier density and e is the electron charge) of the Si(111) 2D system, both for $g_v = 2$ and 6, as functions of temperature and density for several different impurity configurations. The density dependence agrees very well with the unpublished work of Kane,[26] and shows that the disorder in this new batch of Si(111)-vacuum samples is approaching the $\sim 10^{10}\text{cm}^{-2}$ limit which is one to two orders of magnitude lower than the usual Si 2D samples,[1] thus explaining the very high mobilities of these new 2D systems. Our results also demonstrate that the strong screening by the $g_v = 6$ Si(111) system, compared with the $g_v = 2$ system, would lead to much stronger temperature dependence of the conductivity or the mobility, thus providing a clear means to distinguish the valley degeneracy. Our calculated density dependence of the mobility is approximately consistent with the recent measurements.[26]

Based on these calculation we can approximately estimate[27] the expected activation energy of the 1/3 fractional quantum Hall state of the Si(111) 2D system (in these high-mobility samples) to be ∼5–10 K using the Zhang-Das Sarma model[28] (and subtracting out the level broadening effect[27] using our calculated mobility). The observation of the fractional quantum Hall effect in Si(111) 2D system here is only possible because of the incredibly high mobilities achieved through hydrogen passivation, and it is indeed a materials science breakthrough.

V. CONCLUSION

The main purpose of this article is a systematic theoretical investigation of the valley degeneracy effect on 2D electronic transport properties in Si-MOSFET systems. We calculate theoretically charged-impurity scattering-limited 2D electronic transport in Si(100), (110), and (111) inversion layers at low temperatures and carrier densities, where screened charged-impurity scattering is important. The 2D mobility for a given system increases quadratically with increasing valley degeneracy, $\mu \propto \sigma/n \propto g_v^2$, in the strong screening limit ($q_0 = q_{\text{TF}}/2k_F$) for the same impurity configuration. We also show that the temperature and the parallel magnetic field dependence of the 2D conductivity is strongly enhanced by increasing the valley degeneracy. All our results are valid only at carrier densities above which localization effects become important, but we estimate that the transition to the insulating state occurs well below 10^{11} cm^{-2} density in the high mobility systems of our interest[14,15,26] in the current work.

We conclude by emphasizing our findings in both Si-SiO_2 and Si-vacuum MOSFETs. The parallel magnetic field and the temperature dependence of the resistivity (at zero parallel field) manifest strong valley dependence regardless of impurity configurations. For $g_v = 1$ both $\rho(T)$ and $\rho(B_\parallel)$ show weak temperature and magnetic-field dependence by virtue of weak screening, and for $g_v = 6$ due to strong screening (i.e., large $q_0 = q_{\text{TF}}/2k_F$) the resistivity shows both strong temperature and magnetic field dependence. Our finding of remarkably strong valley dependence of 2D transport properties in Si-MOSFETs and the interesting physics of valley-dependent 2D transport should be investigated experimentally. Similar strong valley degeneracy dependence is also apparent in the many-body effects of 2D systems, which have been studied elsewhere.[29] We have also provided detailed calculations for the valley-dependent transport properties of 2D Si(111) systems as a function of temperature and density in very high-mobility low-disorder samples, commenting on the possible activation energy for the fractional quantum Hall effect in such ultraclean Si system.

ACKNOWLEDGMENT

This work was supported by LPS-NSA.

[1] T. Ando, A. B. Fowler, and F. Stern, Rev. Mod. Phys. **54**, 437 (1982).

[2] S. Das Sarma, S. Adam, E. H. Hwang, and E. Rossi, Rev. Mod. Phys. **83**, 407 (2011).

[3] I. Vurgaftman, J. R. Meyer, and L. R. Ram-Mohan, J. Appl. Phys. **89**, 5815 (2001).

[4] H. W. van Kesteren, E. C. Cosman, P. Dawson, K. J. Moore, and C. T. Foxon, Phys. Rev. B **39**, 13426 (1989);

K. Maezawa, T. Mizutani, and S. Yamada, J. Appl. Phys. **71**, 296 (1992).
[5]E. Abrahams, S. V. Kravchenko, and M. P. Sarachik, Rev. Mod. Phys. **73**, 251 (2001).
[6]S. V. Kravchenko and M. P. Sarachik, Rep. Prog. Phys. **67**, 1 (2004).
[7]S. Das Sarma and E. H. Hwang, Solid State Commun. **135**, 579 (2005); Phys. Rev. Lett. **83**, 164 (1999).
[8]B. Spivak, S. V. Kravchenko, S. A. Kivelson, and X. P. A. Gao, Rev. Mod. Phys. **82**, 1743 (2010).
[9]S. V. Kravchenko, G. V. Kravchenko, J. E. Furneaux, V. M. Pudalov, and M. D'Iorio, Phys. Rev. B **50**, 8039 (1994).
[10]G. Zala, B. N. Narozhny, and I. L. Aleiner, Phys. Rev. B **64**, 214204 (2001).
[11]A. Gold and V. T. Dolgopolov, Phys. Rev. B **33**, 1076 (1986).
[12]A. Punnoose and A. M. Finkelstein, Phys. Rev. Lett. **88**, 016802 (2001); Science **310**, 289 (2005).
[13]D. C. Tsui and G. Kaminsky, Solid State Commun. **20**, 93 (1976).
[14]K. Eng, R. N. McFarland, and B. E. Kane, Appl. Phys. Lett. **87**, 052106 (2005); Physica E **34**, 701 (2006).
[15]K. Eng, R. N. McFarland, and B. E. Kane, Phys. Rev. Lett. **99**, 016801 (2007); B. Hu, T. M. Kott, R. McFarland, and B. E. Kane, Appl. Phys. Lett. **100**, 252107 (2012).
[16]E. H. Hwang and S. Das Sarma, Phys. Rev. B **75**, 073301 (2007).
[17]A. Gold, Phys. Rev. B **82**, 195329 (2010).
[18]A. Gold, L. Fabie, and V. T. Dolgopolov, Appl. Phys. Lett. **91**, 052112 (2007); Physica E **40**, 1351 (2008).
[19]L. J. Sham and M. Nakayama, Surf. Sci. **73**, 272 (1978); Phys. Rev. B **20**, 734 (1979).
[20]L. A. Tracy, E. H. Hwang, K. Eng, G. A. Ten Eyck, E. P. Nordberg, K. Childs, M. S. Carroll, M. P. Lilly, and S. Das Sarma, Phys. Rev. B **79**, 235307 (2009).
[21]G. D. Mahan, *Many Particle Physics* (Plenum Publisher, New York, 2000).
[22]W. E. Howard and F. F. Fang, Phys. Rev. B **13**, 2519 (1976).
[23]V. T. Dolgopolov and A. Gold, JETP Lett. **71**, 27 (2000); I. F. Herbut, Phys. Rev. B **63**, 113102 (2001).
[24]S. Das Sarma and E. H. Hwang, Phys. Rev. B **72**, 035311 (2005).
[25]S. Das Sarma and E. H. Hwang, Phys. Rev. Lett. **84**, 5596 (2000).
[26]Tomasz M. Kott, Binhui Hu, S. H. Brown, and B. E. Kane, arXiv:1210.2386; B. E. Kane (private communication).
[27]C. R. Dean, B. A. Piot, P. Hayden, S. Das Sarma, G. Gervais, L. N. Pfeiffer, and K. W. West, Phys. Rev. Lett. **100**, 146803 (2008).
[28]F. C. Zhang and S. Das Sarma, Phys. Rev. B **33**, 2903 (1986).
[29]S. Das Sarma, E. H. Hwang, and Q. Li, Phys. Rev. B **80**, 121303 (2009).